Impact of matching network on the capacity of compact MIMO systems

Lau, Buon Kiong; Bach Andersen, Jørgen; Kristensson, Gerhard; Molisch, Andreas

Published in:
Antenn 06 - The Nordic Antenna Symposium

2006

IMPACT OF MATCHING NETWORK ON THE CAPACITY OF COMPACT MIMO SYSTEMS

Buon Kiong Lau[1], Jørgen Bach Andersen[2], Gerhard Kristensson[1], and Andreas F. Molisch[1,3]

[1] Department of Electroscience, Lund University, SE-221 00 Lund, Sweden
Buon-Kiong.Lau@es.lth.se, Gerhard.Kristensson@es.lth.se

[2] Department of Communication Technology, Aalborg University, DK-9220 Aalborg, Denmark
jba@kom.auc.dk

[3] Mitsubishi Electric Research Laboratories, Cambridge, MA 02139 USA
Andreas.Molisch@ieee.org

ABSTRACT

MIMO is an undisputed breakthrough in advanced wireless technology, as it offers potentially linear increase in information-theoretic capacity with the number of antennas. However, the implementation of MIMO in compact terminals is a relatively uncharted topic, due to challenging problems with high antenna correlation and mismatch loss, both of which greatly reduces the expected MIMO gains. In this paper, we investigate the remedial impact of matching networks on the capacity degradation in such systems with respect to both uniform 2D angular power spectrum and measured wideband outdoor-to-indoor channels. We find that the optimum narrowband multiport-matching network can perform poorly in the wideband case. For a modest 2.3% fractional bandwidth, the narrowband and wideband capacities (per unit bandwidth) can differ by as much as 60%. The multipath richness of the propagation scenario is also shown to have an important effect on the benefits that can be derived from more sophisticated matching networks which take into account mutual coupling in their designs.

1. INTRODUCTION

Until a few years ago, antenna arrays were only considered for implementation at the base station (BS), due to the asymmetrical data traffic and requirement for low complexity/power in the mobile stations (MSs) [1], [2]. However, in order to achieve further performance gains, such as those afforded by MIMO systems [3]-[6], antenna arrays must also be incorporated into the MSs.

While antennas at the BS can be sufficiently separated to minimize spatial correlation and electromagnetic (or mutual) coupling, this is not feasible for the ever smaller MSs. The effect of high antenna correlation resulting from sampling closely separated spatial points is well known [7]. Whereas mutual coupling can reduce antenna correlation by introducing diversity in the antenna patterns, it also increases impedance mismatch and thus decreases antenna efficiency. By a proper design of matching networks, much of the performance loss can be recovered. However, the tradeoffs are narrower frequency bandwidths for *both* correlation and efficiency [8].

In an earlier paper [9], we considered the impact of matching network on the wideband capacity of compact 2×2 MIMO systems. Unfortunately, the 3GPP-3GPP2 spatial channel model [10] can only offer a relatively narrow bandwidth of 5 MHz, which translates to a fractional bandwidth of 0.25% at the 2 GHz operating frequency. Therefore, the impact of narrow correlation and efficiency bandwidths resulted in only a modest degradation in wideband capacity. Moreover, only one propagation scenario (i.e. "urban microcell") was investigated.

In the present contribution, we extend our study to three propagation scenarios: uniform 2D angular power spectrum (APS); a line-of-sight (LOS) and a non-LOS scenario from measured outdoor-to-indoor channels [11]. Specifically, the measured channels give a bandwidth of 120 MHz at 5.2 GHz (or fractional bandwidth of 2.3%). In addition to the three matching conditions studied in [9], we also consider the recently introduced *input impedance match* [12], an individual-port match which facilitates low correlation by complex conjugate matching of the input impedance.

2. MIMO SYSTEM MODEL

Figure 1 presents the simplified model of a $M \times N$ (or 2×2) MIMO system. We assume downlink transmission, though the model is equally applicable for the uplink by reciprocity. The transmit and receive antenna arrays and the scatterers are assumed to be in the farfield of one another. For convenience, we do not explicitly show the frequency dependence of system parameters.

2.1. Transmit and Receive Subsystem

In the transmit subsystem (or BS), a voltage source V_{Si} with a source impedance Z_{Si} is connected across the input of the j-th dipole antenna. The two antennas, separated by a distance d, is represented by a 2×2 impedance matrix $\mathbf{Z}_{TT}$, where for identical dipoles and $Z_{ij} = [\mathbf{Z}_{TT}]_{ij}$, $Z_{11} = Z_{22}$ ($Z_{21} = Z_{12}$ by reciprocity). The radiated field of the j-th antenna may be deduced from $\mathbf{Z}_{TT}$ and the open-circuit fields $e_j^{T}(\theta)$'s, which are obtained from method-of-moments (MoM) implementation of [13].

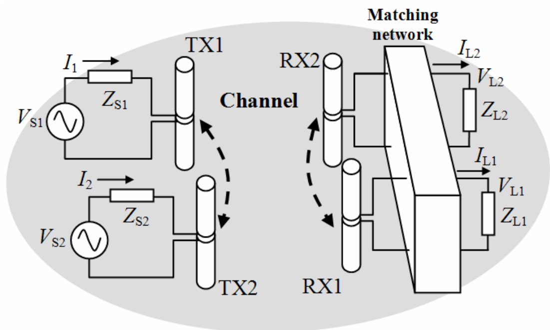

Figure 1. A 2×2 MIMO communication system: Transmit subsystem, propagation channel and receive subsystem. Dashed lines with arrowheads represent mutual coupling.

The receive subsystem (or MS) is nearly identical to the transmit subsystem (where in this case the voltage sources are open-circuit voltages across the antenna inputs), except for a 2×2 matching network at the antenna inputs. As with the BS, the induced current per incident field of the i-th antenna is calculated from the impedance matrix of the receive antennas $\mathbf{Z}_{RR}$ and open-circuit induced voltages $E_i^{T}(\theta)$'s, with the latter two obtained from either [13] or the transmit case by reciprocity.

2.2. Propagation Channel

Both a frequency flat channel with uniform azimuthal APS and measured outdoor-to-indoor channels [11] are used for the numerical simulations; in both cases, 2D propagation is modeled, i.e., the elevation spread is neglected. The measured channels provide realistic channel responses in the angle and delay domains. Each realization of the propagation channel is characterized by its multipath components. Specifically, θ_l^{D}, θ_l^{A}, β_l, and τ_l are respectively the direction-of-departure (DOD), direction-of-arrival (DOA), complex gain and delay of the l-th multipath component (MPC).

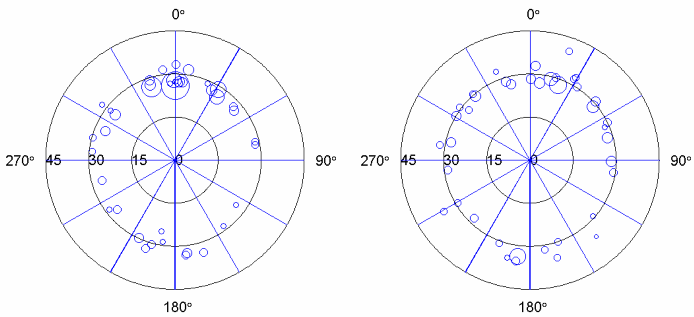

Fig. 2. DOA-delay plot in azimuth plane for (a) LOS and (b) NLOS positions. The sizes of circles indicate the powers of the MPCs (in linear scale). Radial axis in meters (with the delays expressed as the total distances traversed by the MPCs). North of the site map (see Fig. 5 in [11]) and broadside of the dipole array correspond to 0°.

The outdoor-to-indoor measurement campaign [11] was performed at the "E-building" of LTH, Lund University, Sweden. In total, 159 measurements were made for 3 transmit positions (Tx1-Tx3) and 53 receive positions in the offices and corridor. For each transmit-receive position pair, the SAGE algorithm was used to extract $N_p = 40$ MPCs from 13 MIMO snapshots. For our study, we selected two representative receive positions (for Tx1) in Room 2334 (see Fig. 5 in [11]): (1) a LOS position with the receiver in the middle of the room, RMS angular spread of 30°, RMS delay spread of 5.2 ns, and 95.8% captured power at a SNR of 19.2 dB, and (2) a non-LOS (NLOS) position with receiver to the west of the LOS position, RMS angular spread of 52.3°, RMS delay spread of 8.2 ns, and 88.7% captured power at a SNR of 15.1 dB. The extracted MPCs are illustrated in Fig. 2(a) and 2(b).

3. S-PARAMETER MODELING

Although the Z-parameter representation is often used to represent the communication blocks in Fig. 1, it is convenient to use the S-parameter representation for capacity calculations [14]. The Z- and S-parameter matrices are related by the transformation $\mathbf{S} = \mathcal{F}(\mathbf{Z}) = \left(\mathbf{Z} + Z_0\mathbf{I}\right)^{-1}\left(\mathbf{Z} - Z_0\mathbf{I}\right)$, where Z_0 = 50Ω is the characteristic impedance. The combined S-matrix of the transmit antennas, channel and receive antennas is given by [14]

$$\mathbf{S}_{\mathrm{H}} = \begin{bmatrix} \mathbf{S}_{\mathrm{TT}} & \mathbf{S}_{\mathrm{RT}} \\ \mathbf{S}_{\mathrm{TR}} & \mathbf{S}_{\mathrm{RR}} \end{bmatrix} \tag{1}$$

where $\mathbf{S}_{\mathrm{RT}} = \left(\mathbf{I} + \mathbf{Z}_{\mathrm{RR}}/Z_0\right)\left(\mathbf{Z}_{\mathrm{RT}}/Z_0\right)\left(\mathbf{I} - \mathbf{S}_{\mathrm{TT}}\right)$ and $\left[\mathbf{Z}_{\mathrm{RT}}\right]_{ij} = \sum_{l=1}^{N_p} E_i^{\mathrm{R}}\left(\theta_l^{\mathrm{A}}\right)\beta_l e_j^{\mathrm{T}}\left(\theta_l^{\mathrm{D}}\right)$, and $\mathbf{S}_{\mathrm{TT}}$ and $\mathbf{S}_{\mathrm{RR}}$ are S-parameter equivalents of $\mathbf{Z}_{\mathrm{TT}}$ and $\mathbf{Z}_{\mathrm{RR}}$. We assume negligible backscattering $\mathbf{S}_{\mathrm{TR}} = \mathbf{0}$. The matching network is represented by

$$\mathbf{S}_{\mathrm{M}} = \begin{bmatrix} \mathbf{S}_{11} & \mathbf{S}_{12} \\ \mathbf{S}_{21} & \mathbf{S}_{22} \end{bmatrix}, \tag{2}$$

We consider only lossless matching network, so that $\mathbf{S}_{\mathrm{M}}^H \mathbf{S}_{\mathrm{M}} = \mathbf{I}$, where superscript H denotes Hermitian transpose. Thus, only $\mathbf{S}_{11}$ and $\mathbf{S}_{22}$ need to be specified, while $\mathbf{S}_{12}$ and $\mathbf{S}_{21}$ are obtained from

$$\mathbf{S}_{11}^H \mathbf{S}_{11} + \mathbf{S}_{21}^H \mathbf{S}_{21} = \mathbf{I} \text{ and } \mathbf{S}_{12}^H \mathbf{S}_{12} + \mathbf{S}_{22}^H \mathbf{S}_{22} = \mathbf{I}. \tag{3}$$

In this paper, we calculate $\mathbf{S}_{12}$ and $\mathbf{S}_{21}$ from Cholesky factorization.

3.1. Matching Conditions

As in [9], we evaluate the capacity performance for the characteristic impedance (or Z_0) match, the self impedance match and the multiport conjugate match. The details are given in [9]. In addition, we also investigate the *input impedance match* [12]. Although the observation that zero correlation can be achieved in uniform 3D APS for closely coupled antennas with individual port matching can be traced to earlier publications [15], [16], it was first formalized in [12] and [17]. A recent publication demonstrates the interesting results that the input impedance match maximizes the effective diversity gain for two closely coupled dipoles in uniform 3D APS [18].

Unlike the self impedance match, which only takes into account the self impedance of the antenna, the input impedance match also takes into account mutual coupling. The input impedance match attempts to conjugate-match the antenna pair individually (one at a time), i.e., there is a separate matching network for each port, and the Z-matrix of the matching network is diagonal. In essence, this is equivalent to the receive subsystem in Fig. 1 without the matching network and the loads being used as matching impedances. It has been shown that the input impedance match is obtained when the antenna input impedance is the complex conjugate of the load impedance as seen by each antenna input, i.e. $Z_{\mathrm{in}} = Z_{\mathrm{L}}^*$ [12]. The solution can be obtained either iteratively or algebraically (in a closed form). For identical dipole antennas $Z_{11} = Z_{22}$, the unique solution is given by [12]

$$Z_{\mathrm{L}}^{\mathrm{opt}} = \sqrt{R_{11}^2 - R_{12}^2 + X_{12}^2 - (R_{12}^2 X_{12}^2)/R_{11}^2} + j\left((R_{12}X_{12})/R_{11} - X_{11}\right), \tag{4}$$

where $Z_{11} = R_{11} + jX_{11}, Z_{12} = R_{12} + jX_{12}$. Note that whereas the input impedance match facilitates maximum power transfer from the single excited voltage source into the corresponding antenna port, it gives no consideration to power coupled into adjacent antenna(s). In fact, it has been found that the input impedance match does not give maximum received power for individual-port matching [19]. It is shown in [19] that the individual-port match can be used to maximize received power or minimize antenna correlation in a given propagation environment (or random field).

3.2. Performance Measures

We focus here on wideband capacity performance for unknown channel state information at the transmitter. Corresponding results and discussions for correlation, efficiency and bandwidths are the subjects of [8], [9]. The channel information capacity for the 2 × 2 MIMO system over a bandwidth B (in bits/s/Hz) is [9], [14]

$$C = \frac{1}{B}\int_B \log_2\left\{\det\left(\mathbf{I} + \frac{P_\mathrm{T}}{2B\sigma_n^2}\mathbf{H}(f)\mathbf{H}(f)^H\right)\right\}df\,, \tag{5}$$

where the *overall* channel matrix $\mathbf{H} = \mathbf{\Lambda}_\mathrm{D}^{1/2}\xi_\mathrm{D}^H\mathbf{S}_\mathrm{RT}$ and $Z_0\left(\mathbf{I} - \mathbf{S}_\mathrm{RR}\mathbf{S}_{11}^H\right)^{-1} = \xi_\mathrm{D}\mathbf{\Lambda}_\mathrm{D}^{1/2}\xi_\mathrm{D}^H$, σ_n^2 the receive noise power density (assumed constant over B), and P_T the total transmit power over B.

4. SIMULATION RESULTS

For all three propagation scenarios described in Section 2.2, we perform the capacity analysis over 120 MHz bandwidth with center frequency 5.2 GHz. For the purpose of calculating capacity, we require a large number of realizations of the channel that has the same statistical properties. Therefore, we employ the "random phase method" to synthetically generate channel realizations from the MPC data for a given transmit-receive position [20]. The mean capacity is obtained from 1000 realizations of the channel for each antenna separation. The Z_0 match no-coupling (nc) case is chosen as the reference case, where for a given P_T, the corresponding average received signal power in B, with the averaging taken over all four transmit-receive channels in **H** and all channel realizations, is calculated. Then, the noise power $B\sigma_n^2$ is determined such that the receive SNR is 10 dB. The same P_T and noise power are then used for all calculations with mutual coupling, including the cases of Z_0 match, self (impedance) match, input (impedance) match and MC match in Figs. 3-5.

4.1. Uniform 2D APS

To investigate the impact of bandwidth on the results, we first consider the narrowband case in Fig. 3(a), where only the mean capacities at the center frequency is calculated. The capacity performance of the Z_0 match no-coupling (nc) case shares a similar trend to that in [14]. Apart from a constant mismatch loss, the mean capacity depends on spatial correlation which in a uniform 2D APS is fully described by the well-known Clarke's formula $J_0(kd)$, where $J_0(\bullet)$ is the zero-th order Bessel function of the first kind and $k = 2\pi/\lambda$ is the wave number. It is obvious from Fig. 3(a) that the capacity performance of Z_0 match *with* coupling is consistently worse than the no-coupling case, which implies that the pattern diversity obtained from coupling fails to offset the increased mismatch loss (cf. Figs. 2 and 3 in [9]).

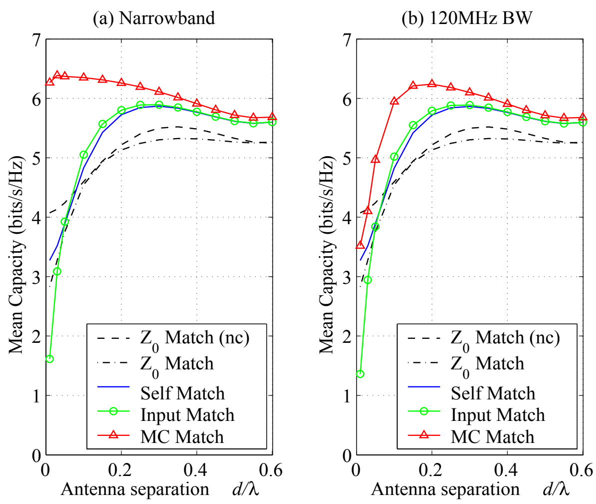

Fig. 3. Mean capacities for different matching conditions at different receive antenna separations in uniform 2D

The self impedance match fares better than the Z_0 match case over the given range of antenna separations. This indicates that a crude attempt at matching the self impedance can bring about mean capacity gains which exceed 0.5 bits/s/Hz for $d \in [0.1\lambda, 0.4\lambda]$. The difference (or gap) in the mean capacities between Z_0 match and self impedance match at larger separations (when mutual impedance is smaller) is due to the penalty in efficiency for the Z_0 match from not matching the self impedance of the antenna. By taking into account mutual coupling, the input impedance match demonstrates marginally superior performance over $d \in [0.05\lambda, 0.3\lambda]$ when compared to the self impedance match. Nevertheless, due to increasingly strong coupling of received power into the adjacent antenna for the input impedance match, the mean capacity falls below that of the self-impedance match for $d < 0.05\lambda$. The good performance of the MC match over the entire range of $d < 0.6\lambda$, as compared to other cases, can be understood from its low correlation and near 100% matching efficiency [8], [9]. The seemingly counter-intuitive trend of increasing mean capacity for MC match with decreasing d (while other mean capacities are decreasing) can be attributed to the power scattered by each receive antenna being recaptured by the adjacent antenna, a phenomenon also observed in [14]. We further note that the mean capacities of the self impedance match, input impedance match and MC match converge to one other at larger antenna separations. This is because the latter two are generalizations of the self impedance match to account for mutual impedance, which decreases at larger antenna separations.

In the corresponding wideband case (see Fig. 3(b)), we observe (except for the MC match) nearly identical trends to those in Fig. 3(a). This is because the bandwidth of 2.3% is still relatively narrow when compared to the bandwidth of dipole antennas. For a single dipole antenna, the bandwidth for self-impedance match is as high as 17.8% for a –6 dB return loss [8]. For the MC match, it is obvious that wideband mean capacity suffers severe degradation as compared to the narrowband case, particularly for $d < 0.1\lambda$. For example, the capacity drops from 6.3 to 5 bits/s/Hz at $d = 0.05\lambda$. This is the direct result of narrow correlation and efficiency bandwidths that are the price being paid for obtaining good performance at the center frequency [8].

4.2. NLOS scenario

For the NLOS scenario that has moderate angular and delay spreads (Figs. 4(a) and (b)), we observe that the loss of multipath richness (thus increased correlation) in the channel causes an expected downward shift in all the capacity curves, as compared to Figs. 3(a) and (b). The capacity degradation is highest for the MC match, and it is as high as 1.8 bits/s/Hz for small antenna separations. As before, the narrowband and wideband capacities in Figs. 4(a) and (b) only differ for the MC match. Unlike the uniform 2D APS, the input impedance match no longer has an advantage over the self-impedance match. For $d < 0.1\lambda$, the self impedance match clearly provides the better match.

4.3. LOS scenario

The capacity results of the LOS scenario in Figs. 5(a) and (b) continue the downward trend in Figs. 4(a) and (b), due to even smaller angular and delay spreads. In this case, the input impedance match has worse capacity performance than self impedance match for $d < 0.2\lambda$. It is interesting to note that the wideband capacity of the MC match in Fig. 5(b) falls below that of the Z_0 match with no coupling for $d < 0.2\lambda$, indicating that in an environment with low multipath richness, mutual coupling effects cannot be fully compensated by the conventional narrowband matching networks. Indeed, it is observed in Fig. 5(b) that in such an environment, different matching techniques do not produce significantly different capacity performances.

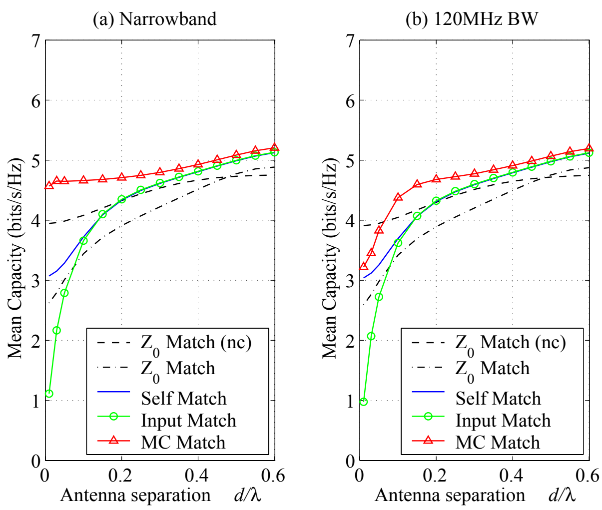

Fig. 4. Mean capacities for different matching conditions at different receive antenna separations in NLOS scenario.

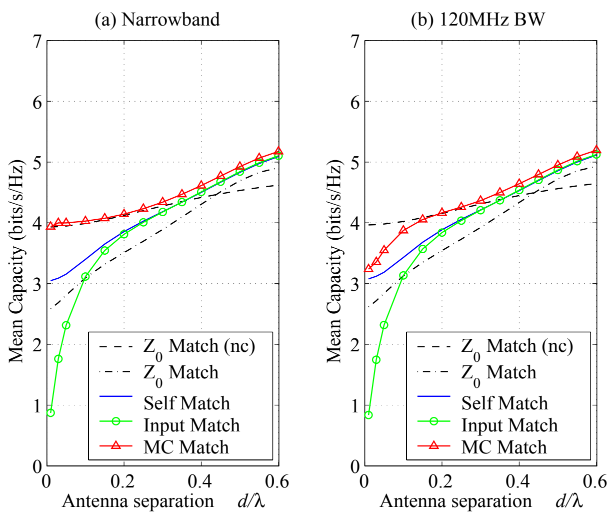

Fig. 5. Mean capacities for different matching conditions at different receive antenna separations in LOS scenario.

5. CONCLUSIONS

In the paper, the matching network is shown to play a significant role in determining the wideband capacity performance of MIMO systems. The benefits that are brought about by MC match, which is optimum for the multiple antenna configurations in the narrowband case, can become insignificant for wideband systems. As a case in point, for uniform 2D APS and $d = 0.03\lambda$, the capacity decreases from the narrowband case of 6.4 to the 2.3% bandwidth case of 4 bits/s/Hz, which represents a steep 60% drop! On the other hand, in propagation scenarios characterized by lower angular spread, the bandwidth has a less significant effect on the capacity performance of the MC match. Finally, we have limited the scope of our study to narrowband matching, where only the antenna impedances at the center frequency are used in the design process. Thus, an interesting area for future work is the study of wideband matching networks for compact MIMO systems.

ACKNOWLEDGMENT

We thank Shurjeel Wyne and Gunnar Eriksson for supplying the processed data from the outdoor-to-indoor measurement campaign [11]. Part of this work was financially supported by the VINNOVA under grant no. P24843-3, and an INGVAR grant from SSF.

REFERENCES

[1] S. Andersson, B. Hagerman, H. Dam, U. Forssén, J. Karlsson, F. Kronestedt, S. Mazur, and K. J. Molnar, "Adaptive antennas for GSM and TDMA systems," *IEEE Personal Commun.*, vol. 6., no. 3, pp. 74-86, Jun. 1999.

[2] B. K. Lau, M. Berg, S. Andersson, B. Hagerman, and M. Olsson, "Performance of an adaptive antenna system in EGPRS networks," in *Proc. IEEE VTC-Spring*, vol. 4, pp. 2354-2358, Rhodes, Greece, 6-9 May 2001.

[3] J. Winters, "On the Capacity of Radio Communication Systems with Diversity in a Rayleigh Fading Environment," *IEEE J. Select. Areas Commun.*, vol. SAC-5, pp.871-878, Jun. 1987.

[4] I. E. Telatar, "Capacity of multi-antenna Gaussian channels," *European Trans. Telecommun.*, vol. 10, pp. 585-595, 1999.

[5] G. J. Foschini and M. J. Gans, "On limits of wireless communications in a fading environment when using multiple antennas," *Wireless Personal Communications* (Kluwer Academic Publishers), vol. 6, pp. 311–335, Mar. 1998.

[6] A. F. Molisch, *Wireless Communications*, John Wiley and Sons, 2005, ch. 20.

[7] D. S. Shiu, G. J. Foschini, M. J. Gan, J. M. Kahn, "Fading correlation and its effect on the capacity of multielement antenna systems," *IEEE Trans. Commun.*, vol. 48, pp. 502-513, Mar. 2000.

[8] B. K. Lau, J. B. Andersen, G. Kristensson, and A. F. Molisch, "Impact of matching network on bandwidth of compact antenna arrays," *IEEE Trans. Antennas Propagat.*, to appear Jul. 2006.

[9] B. K. Lau, S. M. S. Ow, G. Kristensson, and A. F. Molisch, "Capacity analysis for compact MIMO systems", in *Proc. IEEE VTC Spring*, vol. 1, pp. 165-170, Stockholm, Sweden, 30 May- 1 Jun. 2005.

[10] 3GPP-3GPP2 ad-hoc Spatial Channel Modeling Group, "MIMO channel model", v.6.0 Document 134, http://www.3gpp.org/ftp/tsg_ran/WG1_RL1/3GPP_3GPP2_SCM/.

[11] S. Wyne, P. Almers, G. Eriksson, J. Kåredal, F. Tufvesson, and A. F. Molisch, "Outdoor to indoor office MIMO measurements at 5.2 GHz," in *Proc. IEEE 60th VTC Fall*, vol. 1, pp. 101-105, Los Angeles, CA, 26-29 Sep. 2004.

[12] S. M. S. Ow, "Impact of mutual coupling on compact MIMO systems," M.Sc. Thesis, Dept. Electroscience, Lund University, Lund, Sweden, Mar. 2005. Available: http://www.es.lth.se/teorel/Publications/TEAT-5000-series/TEAT-5074.pdf.

[13] S. N. Makarov, *Antenna and EM Modeling with MATLAB®*, Wiley-Interscience, 2002.

[14] J. W. Wallace and M. A. Jensen, "Mutual coupling in MIMO wireless systems: a rigorous network theory analysis," *IEEE Trans. Wireless Commun*., vol. 3, pp. 1317-1325, Jul. 2004.

[15] A. Derneryd and G. Kristensson, "Multiple antenna signal correlation using near field and far field parameters," in *COST 273*, TD(04) 127, Gothenburg, Sweden, 9-10 Jun. 2004.

[16] S. Dossche, S. Blanch, and J. Romeu, "Optimum antenna matching to minimise signal correlation on a two-port antenna diversity system," *Electron. Lett*., vol. 40, no. 19, pp. 1164-1165, 16 Sep. 2004.

[17] B. K. Lau, J. B. Andersen, G. Kristensson, and A. F. Molisch, "On Impedance Matching and Bandwidth of Compact Antenna Arrays," in *COST 273*, TD(05) 097, Lisbon, Portugal, 10-11 Nov. 2005.

[18] K. Rosengren, J. Carlsson, and P. S. Kildal, "Maximizing the effective diversity gain of two parallel dipoles by optimizing the source impedances," *Microwave Opt. Tech. Lett.*, vol. 48, no. 3, pp. 532-535, Mar. 2006.

[19] J. B. Andersen and B. K. Lau, "On closely coupled dipoles in a random field," *IEEE Antennas and Wireless Propagat. Lett.*, vol. 5, no. 1, pp. 73-75, 2006.

[20] A. F. Molisch, M. Steinbauer, M. Toeltsch, E. Bonek, and R. S. Thoma, "Capacity of MIMO systems based on measured wireless channels," *IEEE J. Select. Areas Commun.*, vol.20, no. 3, pp. 561-569, Apr. 2002.